Rebaudioside B exerts protective effect against experimental autoimmune encephalomyelitis through inhibition of mitochondrial apoptosis pathway

Ning Liu
Lanzhou University Second Hospital
MengJiao Sun
Lanzhou University Second Hospital
Jing Sun
Lanzhou University Second Hospital
PanPan Gong
Lanzhou University Second Hospital
WenJing Zhang
Lanzhou University Second Hospital
HongXia Wang
Lanzhou University Second Hospital
ManXia Wang (wmx322@aliyun.com)
Lanzhou University Second Hospital

Research Article

Keywords: Microglia, Rebaudioside B, Apoptotic, Experimental autoimmune encephalomyelitis

Posted Date: April 6th, 2022

DOI: https://doi.org/10.21203/rs.3.rs-1508282/v1

Abstract

Background:Multiple sclerosis (MS) is one of the major diseases that threaten human health.This study aimed to evaluate the effect and mechanisms of action of Rebaudioside B (Reb B) in the treatment of MS.

Methods: Lipopolysaccharide (LPS) was used to induce an inflammatory response in BV2 microglial cells, which simulates an in vitro MS model.Reb B was screened from small molecular libraries using CCK8 assay and BAX kit. The morphology and functional changes in the LPS- induced BV2 cells were analyzed using the Hoechst 33258 fluorescence staining assay and Western blot (WB).In addition, we established the experimental autoimmune encephalomyelitis (EAE) model of MS in female C57BL/6 mice.We then assessed the clinical symptoms of the EAE mice, and analyzed changes in the expression of key proteins in signal transduction pathways by histopathological staining and WB.

Results: Our data showed that the cell viability in the LPS+Reb B group was highest after administration of 10μM Reb B.Compared with the control group, the apoptotic rate, the Bax/Bcl-2 ratio and the expression of cleavage caspase-3 were significantly increased in the BV2 cells under LPS exposure, a finding that contrasted the trend in the Reb B intervention model group. In the EAE model,there was improvement of clinical symptom scores in the drug treatment group.In addition,histological assessment demonstrated that there was less inflammatory infiltration and less demyelination area in the treatment group compared to the model group.

Conclusion: Taken together,our data demonstrated that Reb B offers protective effect against EAE microglia through inhibition of an apoptotic pathway.

Introduction

Multiple Sclerosis (MS) is an autoimmune disease that causes inflammatory damage to the central nervous system (CNS), which leads to inflammatory demyelination of neurons in the brain and spinal cord(M, 2014). There are 2 million MS patients in the world. Besides, MS is the main cause of disability among young people worldwide, which leads to huge social and economic burden(Iwanowski and Losy, 2015). To date, the pathogenesis of MS remains unclear. To develop novel and effective treatment methods, there is need to conduct in-depth research on the pathogenesis of MS. At present, the mainstay treatment option for MS involves anti-inflammatory or immune regulation which does not fundamentally prevent disease progression(Quan et al., 2019). In addition, functional characterization of protein molecules in signal transduction pathways in immune responses is an attractive strategy in the development of immunotherapy.

With the development of novel drug screening technologies, research and development of new drugs has shifted from laboratory-based assays to clinical application(Reid et al., 2016). Small molecular compounds with novel structures and diversified synthesis have been screened for treatment of MS(Xu et al., 2019). There are 2697 small molecule drugs with definite structures that are on the market, which

have been ratified by Food and Drug Administration (FDA). Although there are many studies on the prevention and treatment of MS by small molecular compounds, evaluation of the mechanisms of action of the small molecule compounds in modulating the immune system may provide new tools for MS treatment.

Previous studies indicated that the pathogenesis of MS involves many factors such as glial cells, immune response as well as environment and nutritional factors(Quan et al., 2019). As the macrophagic cells of the CNS, microglia encompass major components of the brain innate immune system, which generally is in an inactive and resting state(Cao and He, 2013). Under stimulation by reactive oxygen and harmful metabolites, microglia are activated and polarized into M1 type, which express pro-inflammatory mediators and induce neuroinflammation, thus resulting in apoptosis(Miron and Franklin, 2014). An imbalance of the proportion of M1 and M2 type may be the key factor causing myelin regeneration disorder in the progression of MS. Multiple mechanisms, such as cytotoxicity, apoptosis and oxidative stress, have been shown to mediate brain injury by activated microglia in MS(Dulamea, 2017). Therefore, there is a need to actively find new and effective ways to treat MS.

In this study, we employed BV2 cell line to establish LPS model in vitro. We then used the LPS-BV2 cell model to screen 2697 small molecules with novel structures. CCK8 and BAX kit assays showed that Reb B had strong anti-apoptotic effects on the LPS-BV2 model. We tried to elucidate the mechanism of action of Reb B on BV2 cells under LPS induction. On the other hand, we established an EAE mice model and analyzed their clinical symptoms. We performed histological evaluation on the EAE mice treated with Reb B using H&E and LFB staining, and WB. Besides, we studied mitochondrial apoptosis to investigate whether Reb B would show a similar neuroprotective effect in EAE model subjected to brain injury. This study identified and validated Reb B as an effective treatment for MS.

Materials And Methods

Materials

BV2 cell lines were preserved in the Cuiying Biological Research Department laboratory, at the Second Hospital of Lanzhou University, while small molecular libraries were purchased from Selleck company (USA). Fetal bovine serum (FBS), penicillin and streptomycin were bought from GIBCO (USA), while sugar free Dul-becco's Modified Eagle's Medium (DMEM) was purchased from Solarbio (China). CCK8 kit was acquired from Biosharp (China), while human derived BAX ELISA kit and Hoechst 33258 staining dye solution were bought from Abcam (USA).

Female C57BL/6 mice (aged 6-8 weeks, weighing 18-20 g) were purchased from the Animal Experimental Center of Lanzhou University in Gansu, China. We also acquired MOG p35-55 peptide (CS Bio CS0681), Complete Freund's adjuvant (CFA, Sigma, MO, USA), Heat-killed Mycobacterium tuberculosis H37Ra (Difco Laboratories, Detroit, MI, USA) and Pertussis toxin (Alexis, San Diego, CA, USA). The whole experimental process is as shown in Figure 1.

In vitro experiments

Cell culture

The BV2 cells were routinely cultured in DMEM, supplemented with 10% heat-inactivated FBS, penicillin (100 U/mL) and streptomycin (100 U/mL), which were incubated at 37℃ in a humidified incubator (Thermo Fisher, USA) with 5% CO2 and 95% O2.The culture medium was replaced after every two days(Nam et al., 2018).

LPS-induced model of BV2 neuroinflammation

The BV2 cells were grown to logarithmic growth phase, and then treated with 10 μl LPS. The LPS treatment was performed for 24h to induce inflammation in the BV2 cells(Yan et al., 2018).

Small molecular libraries and chemical screening

Small molecular libraries with structuration and diversity, including 2,697 molecules compounds, were purchased from Selleck company (USA). The BV2 cells were incubated in 96-well plates (5×10^3cell/well), and were cultured in the incubator (37℃ ,5% CO2) for 24h. The 2,697 molecule compounds (up to final concentration of 10μM(Zhan et al., 2019)) were added into 96-well plates containing LPS-BV2 (Figure 2). The cell viability was assessed by CCK8 kit (Biosharp, China), following the manufactures instructions. Optical density (OD) was detected by microplate reader at 450nm wavelength, and was directly proportional to the number of living cells in the culture (Thermo Fisher, USA). The obtained data were expressed as the cell survival rate, which was calculated using the following formula: Cell viability (%) = (ODexperimental-ODblank)/(ODcontrol-ODblank)×100%.

Measurement of BAX activity

The BV2 cell concentration at logarithmic growth phase was adjusted to 5×10^4/L, which were then inoculated in 12-well plates at 1ml per well. This experiment was repeated three times, alongside a control group. Afterwards, LPS-BV2 model was established after cell adhesion, followed by the addition of small molecule compounds. Three groups of BV2 cells were collected into 1.5mL EP tubes, which were then washed in pre-cooled PBS. Thereafter, 100ul of the cell lysate was added to each EP tube and incubated on ice for 30min. Finally, the EP tubes were centrifuged for 15 min at 4℃, 12000rpm. The BAX content was analyzed by ELISA (Abcam, USA), following the manufacturer's instructions. The activity of BAX in each group was compared with that in the control group(Li et al., 2021).

Hoechst 33258 fluorescence staining assay

The BV2 cells in the logarithmic growth phase were inoculated in a 6-well plate (1×10^5cell/well). Thereafter, we established the LPS-BV2 model after cell adhesion, followed by the addition of small molecule compounds. Next, the cells were removed from the incubator and cleaned twice with pre-cooling PBS. After being fixed with 4% paraformaldehyde for 10 minutes, at room temperature, the cells were

cleaned three times with PBS for 5 minutes each time. 10mg/L Hoechst 33258 fluorescent dye was added to each well in darkness and incubated for 10 minutes. We used fluorescence microscopy (Olympus, Japan) to analyze the cell morphology of the apoptotic cells. The number of apoptotic cells in 100 cells was counted under random field of view, which was used to calculate the apoptosis rate. Apoptosis rate=(the number of apoptotic cells/cells)×100%(Sun et al., 2018)

Western blot (WB) analysis

Whole cell lysates from each group was extracted using RIPAlysis buffer (50mMTris, pH=7.4, 1% Triton X-100, 1% sodium deoxycholate, 150mM NaCl, 0.1%SDS, sodiumorthovanadate) with a phosphatase inhibitor. The protein concentrations in the collected supernatants were quantified using the BCA assay. The samples were then stored at -20℃ for later use. The extracted proteins were analyzed on a sodium dodecyl sulfate polyacrylamide gel electrophoresis (SDS-PAGE) and transferred onto 0.45μm polyvinylidene fluoride (PVDF) membranes. The membranes were blocked with blocking reagent（Epizyme Biomedical Technology,China）for 2 hours at room temperature, and then incubated with primary antibodies overnight at 4℃. After washing with TBST, the membranes were incubated with species-specific secondary antibodies coupled to horseradish peroxidase. Finally, Chemiluminescence reagents were added for imprint detection. Thereafter, gel imager (Tanon 5200 Multi) was used to visualize the immunoreactive bands, and then the images were analyzed with IMAGE J (National Institutes of Health, USA). The following primary antibodies were used, anti-Caspase3 (1:2000, Proteintech, China), anti-Cleaved Caspase3 (1:2000, CST, USA), anti-Bcl2 (1:2000, Proteintech, China), rabbit anti-Bax (1:4000, Abcam, USA) and β-actin (1:5000, Proteintech, China).

In vivo experiments

Mice

Mice were kept in specific pathogen-free conditions at room temperature (24±2℃), with alternating light/darkness for 12 hours. The mice had access to food and water ad libitum. The animal experiments in this study were approved by the Animal Protection and Use Committee of Lanzhou University Second Hospital and the local Experimental Ethics Committee(Ethical Number:D2021-315).

EAE induction and evaluation

The mice were randomly categorized into the control group, EAE group, and the Reb B treatment group. EAE was induced by subcutaneous injection of 250μg of myelin oligodendrocyte glycoprotein (MOG) p35-55 peptide in mice. The peptides were dissolved in complete Freund's adjuvant which contained 4 mg/ml heat-killed Mycobacterium tuberculosis H37Ra. On the first two days after immunization, the mice received 500ng of pertussis toxin through intraperitoneal injection. We recorded the weight of the mice daily while the clinical scores were recorded at the beginning of modeling(Bittner et al., 2014). The neurological function was scored according to the following criteria: 0-no paralysis, 1-loss of tail tone, 2-

hindlimb weakness, 3-hindlimb paralysis, 4-severe hindlimb and forelimb paralysis, and 5-moribund or death.

Reb B treatment

The mice were randomly allotted to the control group (n=10), the EAE group (n=10), and the Reb B treatment group (n=10). Reb B was administered daily through intraperitoneal injection for 15 days, starting on the 8th day of EAE induction.

Histological evaluation

On the 15th day after modeling, the spinal cords of the injured mice in each group were collected. Briefly, the mice were anesthetized with 10% chloral hydrate (0.2ml/mouse) and perfused with 4% paraformaldehyde for 0.5h. Thereafter, the spinal cord at the lumbar spine enlargement was dissected and then paraffin embedded. Afterwards, the embedded paraffin block was placed at 4℃ for shaping. We then used a blade machine to cut the paraffin blocks into 5μm paraffin sections. The sections were stained with haematoxylin-eosin (H&E) to assess demyelination and inflammatory lesions. These stained sections were analyzed under an optical microscope. to For assessment of inflammatory infiltration, three spinal cord sections were taken from each mouse, and each sections underwent 5 high-power (400×) field analysis to evaluate myelin loss scores. Finally, the mean value of myelin loss scores in each mouse was calculated(Zhen et al., 2015).

H&E staining inflammation scoring criteria:

0 point: no inflammation,

1 point: inflammatory cells only infiltrate around the blood vessels and meninges,

2 points: a few inflammatory cells infiltrate the parenchyma of the brain or spinal cord (1-10/piece),

3 points: moderate inflammatory cells infiltrate the parenchyma of the brain or spinal cord (11-100/piece),

4 points: numerous inflammatory cells infiltrate the parenchyma of the brain or spinal cord (>100/piece).

WB assay

The total protein content in the spinal cords was extracted and underwent WB analyses as previously described.

Results

High throughput screening of small molecular libraries for viability of LPS-induced BV2 cells

To screen new protective small molecule compounds from small molecular libraries, we used CCK8 assay to analyze the viability of LPS-induced BV2 cells model. This analysis was performed alongside a blank group (without BV2 cells) and a control group (BV2 cells treated with 0.5% DMSO). The data showed that the viability of the LPS model was lower than 90%, compared to the other two groups after 94.67% molecule compound intervention, and only about 1% of the cells had significant improvement in the viability. We also demonstrated the cellular viability of the LPS model under intervention with 2697 small compounds (Figure 3).

Analysis of BAX activity by ELISA

We considered 26 molecular compounds which had a cell viability of the LPS model higher than 90% as secondary compounds. We then employed the BAX kit to analyze the expression of BAX in three groups. Our analysis identified Rebaudioside B (C38H60O18, Reb B), a kind of natural sweetener extracted from leaves of Stevia rebaudiana (Figure 2). The BAX level in the Reb B-treated LPS model was significantly lower than in the LPS model (Figure 4, ***P<0.001, LPS+Reb B group vs. LPS group). However, the BAX level in the Reb B-treated LPS model was higher than that in the control group (Figure 4, #P<0.001, LPS+Reb B group vs. control group).

The Reb B intervention concentration was analyzed by CCK8 assay

We measured the activity of BV2 cells treated with different concentrations (0, 1, 10, 100 and 1000μM) of Reb B in the LPS model using the CCK8 assay. The results demonstrated that a Reb B concentration of 10μM exerted the highest cell viability in the LPS+Reb B group compared with the LPS group (Figure 5, ***P<0.001, LPS+Reb B group vs. LPS group). Compared with the LPS group, cell viability of Reb B at 1000μM was significantly reduced (Figure 5, ###P<0.001, LPS+Reb B group vs. LPS group). These data demonstrated that 10μM was the optimal intervention concentration for Reb B.

The morphological changes of BV2 cells were analyzed by Hoechst 33258 staining

Our data showed that the chromatin of BV2 nucleus in the normal control group was evenly distributed, with uniform light blue fluorescence. However, the chromatin in the BV2 nucleus in the LPS group was pyknotic, which showed intensive blue fluorescence in different degrees (Figure 6A). Thus, compared with the control group, the rate of apoptosis rate in the LPS group was significantly increased (Figure 6B, ***P<0.001, LPS group vs. control group), and the apoptosis rate of LPS+Reb B group was obviously decreased (Figure 6B, ###P<0.001, LPS+Reb B group vs. LPS).

Effect of Reb B on pathological changes and clinical scores in EAE mice

To study the effect of Reb B on apoptosis of the EAE mice, we evaluated hyphology of mice through H&E staining. Compared with the EAE group, our data demonstrated that the number of infiltrated inflammatory cells and the demyelination area were reduced in the treated mice (Figure 7).

In addition, the symptoms of mice in the treatment group were significantly delayed compared to the EAE group, thus reducing the incidence and improving the clinical score (Figure 8). Besides, the weight of the mice in the EAE model decreased, and reached the lowest weight at the 15th day after modeling (Figure 9).

Analysis of the expression of apoptosis-related proteins by WB

To analyze whether Reb B plays an anti-apoptotic role in the LPS model, we employed WB analyses to detect protein expression in apoptotic pathways. Compared with the control group, there was significant upregulation of Caspase 3 in LPS group. After pretreatment with Reb B, the expression of Caspase 3 protein was significantly lower compared to the LPS group, but there was no significant difference in the rate of Bax/Bcl2 (Figure 10).

The expression trend of the three proteins (BAX, Bcl-2 and Caspase 3) in the EAE model was consistent with that in cell experiment. Our findings showed that there was significant increase in the expression of Caspase 3 and the rate of Bax/Bcl2 in the EAE group compared to the control group. Treatment of the EAE group with Reb B led to suppression of the expression of Caspase-3 and the rate of Bax/Bcl2(Figure 11). These results supported the hypothesis that Reb B exert anti-apoptotic effects through inhibition of apoptosis pathway.

Discussion

MS is the most common demyelinating disease in the central nervous system, and occurs in young and middle-aged people. MS is characterized by pathological changes which include neuroinflammatory demyelination and neuronal degeneration. It is also associated with complex and dynamic clinical symptoms and signs, which exert a huge economic burden to the society. At present, most of the treatment options for MS focus on delaying disease progression, and there is no drug to reverse the pathological and demyelination injuries. Previous data has reported that the apoptotic physiological process in microglia is up-regulated under inflammatory state(Fu et al., 2022). Recently, apoptosis has been shown to be associated with neuroinflammatory response of microglia in EAE(Zhang et al., 2018), which promotes the release of microglial inflammatory cytokines. Apoptosis is an important mode of programmed cell death that is strictly controlled by many genes, which plays an important role in regulating intracellular environment and metabolic homeostasis. Under pathological conditions, apoptosis is associated with a variety of diseases, which include tumors and autoimmune diseases(Carneiro and El-Deiry, 2020, Krawczyk et al., 2020). Besides, many studies have shown that apoptosis is involved in neuroinflammatory response and demyelination injury in the acute MS(Maiese, 2021). Previous studies have shown that inhibition of apoptosis can play a protective role in EAE model induced by MOG35-55 peptides(Pan et al., 2021). Our results showed that apoptosis was significantly up-regulated in BV2 inflammatory cell model stimulated by LPS. In addition, apoptosis was dramatically up-regulated in the spinal cord of the EAE mice model.

After establishing the inflammatory model on BV2 cells, we screened the FDA library of compounds using high throughput tools(Xian et al., 2021). Through the CCK8 proliferation assay, we selected Reb B from a pool of 2697 small molecular drug compounds with different structures. Reb B was shown to significantly down-regulate the expression of Bax, apoptosis factor, in the inflammatory model established by BV2 cells(Figure 12).

Reb B belongs to a steviol glycoside-tetracyclic diterpenoid extracted from Compositae plants(Dong and Yang, 2020, Zhang et al., 2019). It is often used as a sweet food additive in food production(Tavarini et al., 2020). Reb B is considered to have other pharmacological activities besides being a sweetener(Dong and Yang, 2020). Our analyses showed that Reb B has antioxidant properties, whose biological activity is closely related to reactive oxygen species. Some previous studies have also shown that Reb B has anti-inflammation, antioxidation, antihyperglycemic and anti-tumor properties. However, data on the functional properties of Reb B remain scant(Bakhshi et al., 2008, Huang et al., 2014, Malki et al., 2014, Nico Moons, 2009). Some studies have shown that isosteviol methyl methoxy ether derivatives, the hydrolysate of stevioside, can induce up-regulation of apoptosis in H1299 cells in human lung cancer.

Apoptosis is regulated by several apoptosis-related genes. For instance, the mitochondrial release of apoptosis pathway can trigger a cascade of reactions involving Caspase family of proteins, resulting in suppression of mitochondrial membrane potential. At the same time, bcl-2 family (pro-apoptotic protein Bax), Cty C, AIF and endoG are activated and released into cells, resulting in irreversible apoptosis(Guo et al., 2015). Besides, other studies have demonstrated that many small molecular compounds can mediate apoptosis(Lv et al., 2019). Our results showed that Reb B can significantly inhibit the expression of caspase-3 and Bax in LPS-BV2 cell model, while bcl-2 can significantly promote the expression of anti-apoptotic proteins. In agreement with the EAE model, the expression of caspase-3 and Bax in spinal cord tissues of Reb B intervention group decreased significantly, while the expression of bcl-2 increased significantly. Therefore, Reb B may reduce clinical symptoms score, inflammatory infiltration and demyelination injury in EAE model by inhibiting mitochondrial apoptosis.

Conclusion

Taken together, our study suggested that Reb B plays a protective role in LPS-BV2 cell inflammation and EAE mice model by inhibiting the physiological process mediating mitochondrial apoptosis. These results lay a theoretical basis for the treatment and clinical application of Reb B in reducing demyelination injury in MS.

Declarations

Acknowledgments

We would like to thank the teachers at the Animal Experimental Center of Lanzhou University Second Hospital and the Home for Researchers www.home-for-researchers.com for expert technical assistance.

Funding: This study was funded by the Key R&D Program of Gansu Province Science and Technology Department (20YF8WA087), Cuiying Scientific and Technological Innovation Program of Lanzhou University Second Hospital (CY2021-MS-A06), and Gansu Provincial International Science and Technology Cooperation Base for Precise Treatment of Neurological Diseases.

Competing Interests:The authors declare no conflict of interest.

Author Contributions: Conception, design of the work and experiment:NL and MJS, analysis,interpretation of the data,drafting of manuscript:JS,PPG,WJZ,HXW. MXW supervised the experiment.All authors approved the final version of the paper.All authors have read and agreed to the published version of the manuscript.

Ethics approval: The animal experiments in this study were approved by the Animal Protection and Use Committee of Lanzhou University Second Hospital and the local Experimental Ethics Committee(Ethical Number:D2021-315).

References

1. Bakhshi, J., Weinstein, L., Poksay, K.S., Nishinaga, B., Bredesen, D.E., and Rao, R.V. (2008). Coupling endoplasmic reticulum stress to the cell death program in mouse melanoma cells: effect of curcumin. Apoptosis *13*, 904-914.
2. Bittner, S., Afzali, A.M., Wiendl, H., and Meuth, S.G. (2014). Myelin oligodendrocyte glycoprotein (MOG35-55) induced experimental autoimmune encephalomyelitis (EAE) in C57BL/6 mice. J Vis Exp.
3. Cao, L., and He, C. (2013). Polarization of macrophages and microglia in inflammatory demyelination. Neurosci Bull *29*, 189-198.
4. Carneiro, B.A., and El-Deiry, W.S. (2020). Targeting apoptosis in cancer therapy. Nat Rev Clin Oncol *17*, 395-417.
5. Dong, J., and Yang, Z. (2020). Characterization of a new hemihydrate rebaudioside B crystal having lower aqueous solubility. Food Chem *304*, 125444.
6. Dulamea, A.O. (2017). Role of Oligodendrocyte Dysfunction in Demyelination, Remyelination and Neurodegeneration in Multiple Sclerosis. Adv Exp Med Biol *958*, 91-127.
7. Fu, C., Shuang, Q., Liu, Y., Zeng, L., and Su, W. (2022). Baihe Extracts Reduce the Activation and Apoptosis of Microglia in the Hippocampus of Mice with Depression-like Behaviors by Downregulating MYC. ACS Chem Neurosci *13*, 587-598.
8. Guo, H., Chen, L., Cui, H., Peng, X., Fang, J., Zuo, Z., Deng, J., Wang, X., and Wu, B. (2015). Research Advances on Pathways of Nickel-Induced Apoptosis. Int J Mol Sci *17*.

9. Huang, T.J., Chou, B.H., Lin, C.W., Weng, J.H., Chou, C.H., Yang, L.M., and Lin, S.J. (2014). Synthesis and antiviral effects of isosteviol-derived analogues against the hepatitis B virus. Phytochemistry *99*, 107-114.
10. Iwanowski, P., and Losy, J. (2015). Immunological differences between classical phenothypes of multiple sclerosis. Journal of the Neurological Sciences *349*.
11. Krawczyk, A., Miśkiewicz, J., Strzelec, K., Wcisło-Dziadecka, D., and Strzalka-Mrozik, B. (2020). Apoptosis in Autoimmunological Diseases, with Particular Consideration of Molecular Aspects of Psoriasis. Med Sci Monit *26*, e922035.
12. Li, Y.N., Ning, N., Song, L., Geng, Y., Fan, J.T., Ma, C.Y., and Jiang, H.Z. (2021). Derivatives of Deoxypodophyllotoxin Induce Apoptosis through Bcl-2/Bax Proteins Expression. Anticancer Agents Med Chem *21*, 611-620.
13. Lv, R., Du, L., Zhang, L., and Zhang, Z. (2019). Polydatin attenuates spinal cord injury in rats by inhibiting oxidative stress and microglia apoptosis via Nrf2/HO-1 pathway. Life Sci *217*, 119-127.
14. M, H.D. (2014). In the clinic. Multiple sclerosis. Annals of internal medicine *160*.
15. Maiese, K. (2021). Novel Insights for Multiple Sclerosis and Demyelinating Disorders with Apoptosis, Autophagy, FoxO, and mTOR. Curr Neurovasc Res *18*, 169-171.
16. Malki, A., Laha, R., and Bergmeier, S.C. (2014). Synthesis and cytotoxic activity of MOM-ether analogs of isosteviol. Bioorg Med Chem Lett *24*, 1184-1187.
17. Miron, V.E., and Franklin, R.J. (2014). Macrophages and CNS remyelination. J Neurochem *130*, 165-171.
18. Nam, H.Y., Nam, J.H., Yoon, G., Lee, J.Y., Nam, Y., Kang, H.J., Cho, H.J., Kim, J., and Hoe, H.S. (2018). Ibrutinib suppresses LPS-induced neuroinflammatory responses in BV2 microglial cells and wild-type mice. J Neuroinflammation *15*, 271.
19. Nico Moons, W.D.B., Wim Dehaen (2009). Stevioside and Steviol as Starting Materials in Organic Synthesis. Current Organic Chemistry.
20. Pan, R.Y., Kong, X.X., Cheng, Y., Du, L., Wang, Z.C., Yuan, C., Cheng, J.B., Yuan, Z.Q., Zhang, H.Y., and Liao, Y.J. (2021). 1,2,4-Trimethoxybenzene selectively inhibits NLRP3 inflammasome activation and attenuates experimental autoimmune encephalomyelitis. Acta Pharmacol Sin *42*, 1769-1779.
21. Quan, M.-Y., Song, X.-J., Liu, H.-J., Deng, X.-H., Hou, H.-Q., Chen, L.-P., Ma, T.-Z., Han, X., He, X.-X., Jia, Z., and Guo, L. (2019). Amlexanox attenuates experimental autoimmune encephalomyelitis by inhibiting dendritic cell maturation and reprogramming effector and regulatory T cell responses. BioMed Central *16*.
22. Reid, B.G., Stratton, M.S., Bowers, S., Cavasin, M.A., Demos-Davies, K.M., Susano, I., and McKinsey, T.A. (2016). Discovery of novel small molecule inhibitors of cardiac hypertrophy using high throughput, high content imaging. J Mol Cell Cardiol *97*, 106-113.
23. Sun, D., Xue, A., Xue, X., Ren, M., Wu, J., and Wang, R. (2018). Acetylpuerarin protects against OGD-induced cell injury in BV2 microglia by inhibiting HMGB1 release. Pharmazie *73*, 92-97.

24. Tavarini, S., Clemente, C., Bender, C., and Angelini, L.G. (2020). Health-Promoting Compounds in Stevia: The Effect of Mycorrhizal Symbiosis, Phosphorus Supply and Harvest Time. Molecules*25*.
25. Xian, M., Cai, J., Zheng, K., Liu, Q., Liu, Y., Lin, H., Liang, S., and Wang, S. (2021). Aloe-emodin prevents nerve injury and neuroinflammation caused by ischemic stroke via the PI3K/AKT/mTOR and NF-κB pathway. Food Funct*12*, 8056-8067.
26. Xu, H., Cheng, M., Chi, X., Liu, X., Zhou, J., Lin, T., and Yang, W. (2019). High-Throughput Screening Identifies Mixed-Lineage Kinase 3 as a Key Host Regulatory Factor in Zika Virus Infection. J Virol*93*.
27. Yan, A., Liu, Z., Song, L., Wang, X., Zhang, Y., Wu, N., Lin, J., Liu, Y., and Liu, Z. (2018). Idebenone Alleviates Neuroinflammation and Modulates Microglial Polarization in LPS-Stimulated BV2 Cells and MPTP-Induced Parkinson's Disease Mice. Front Cell Neurosci*12*, 529.
28. Zhan, T., Ambrosi, G., Wandmacher, A.M., Rauscher, B., Betge, J., Rindtorff, N., Häussler, R.S., Hinsenkamp, I., Bamberg, L., Hessling, B.*, et al.* (2019). MEK inhibitors activate Wnt signalling and induce stem cell plasticity in colorectal cancer. Nat Commun*10*, 2197.
29. Zhang, C.J., Jiang, M., Zhou, H., Liu, W., Wang, C., Kang, Z., Han, B., Zhang, Q., Chen, X., Xiao, J.*, et al.* (2018). TLR-stimulated IRAKM activates caspase-8 inflammasome in microglia and promotes neuroinflammation. J Clin Invest*128*, 5399-5412.
30. Zhang, S.S., Chen, H., Xiao, J.Y., Liu, Q., Xiao, R.F., and Wu, W. (2019). Mutations in the uridine diphosphate glucosyltransferase 76G1 gene result in different contents of the major steviol glycosides in Stevia rebaudiana. Phytochemistry*162*, 141-147.
31. Zhen, C., Feng, X., Li, Z., Wang, Y., Li, B., Li, L., Quan, M., Wang, G., and Guo, L. (2015). Suppression of murine experimental autoimmune encephalomyelitis development by 1,25-dihydroxyvitamin D3 with autophagy modulation. J Neuroimmunol*280*, 1-7.

Figures

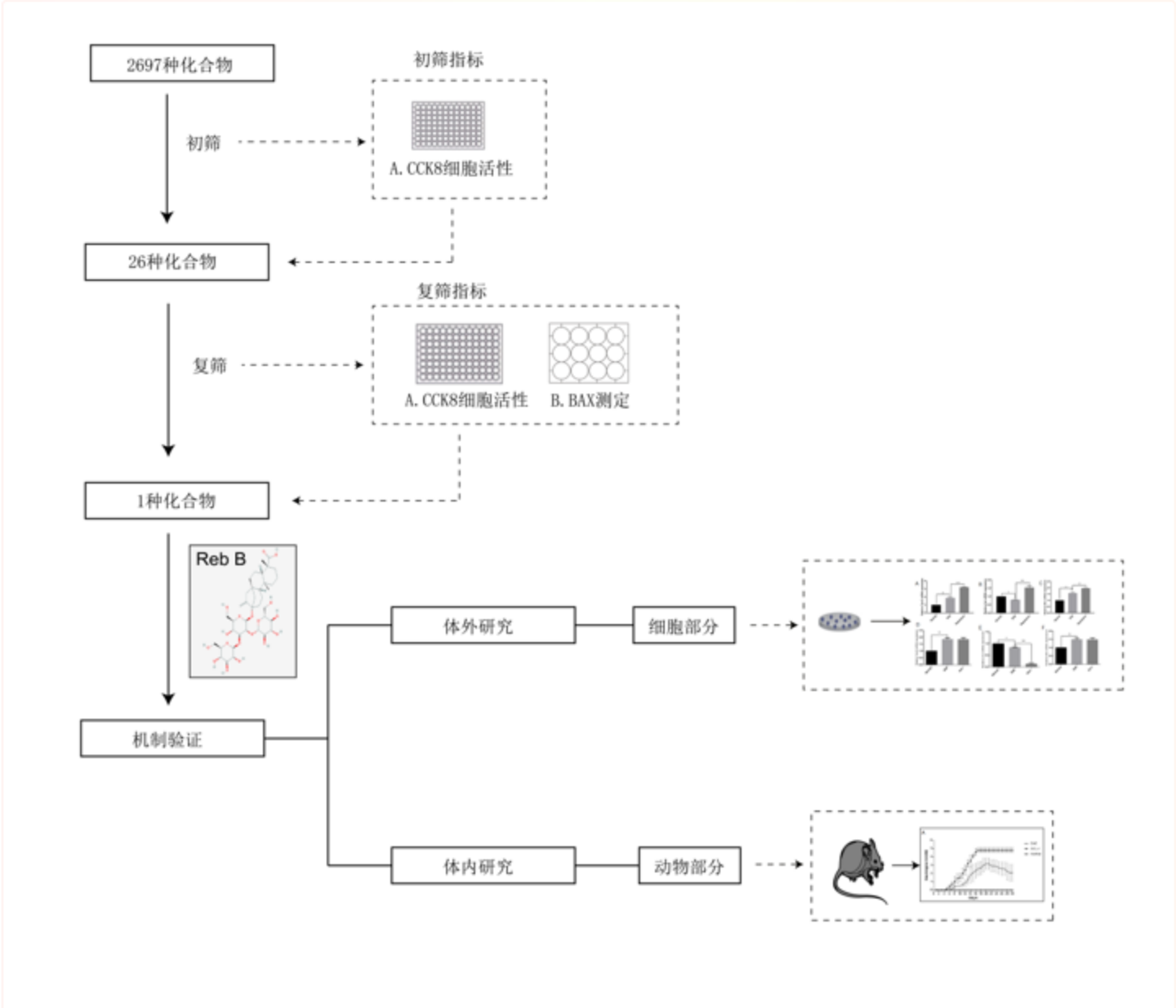

Figure 1

The flow chart of the study

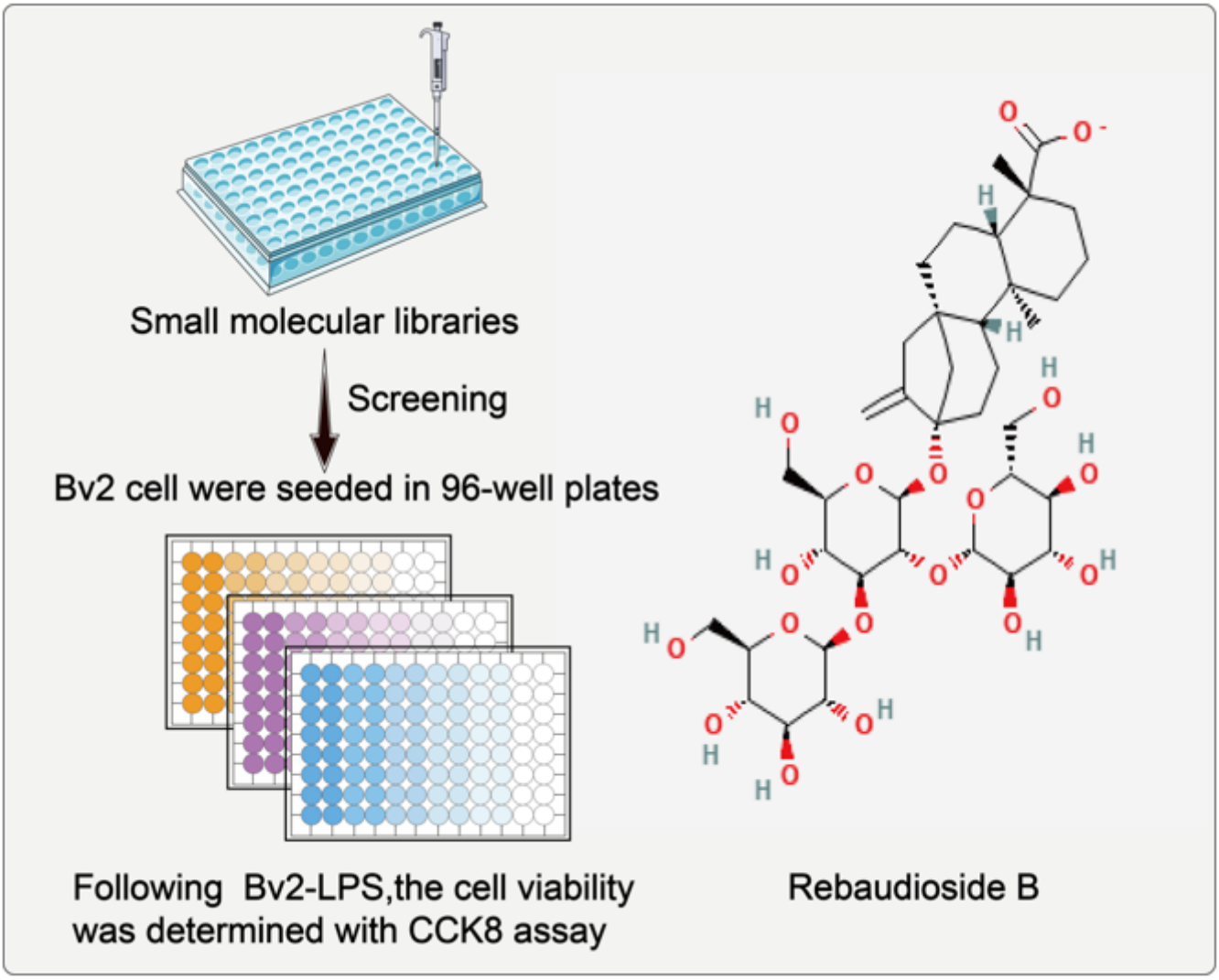

Figure 2

Screening of small molecule compounds

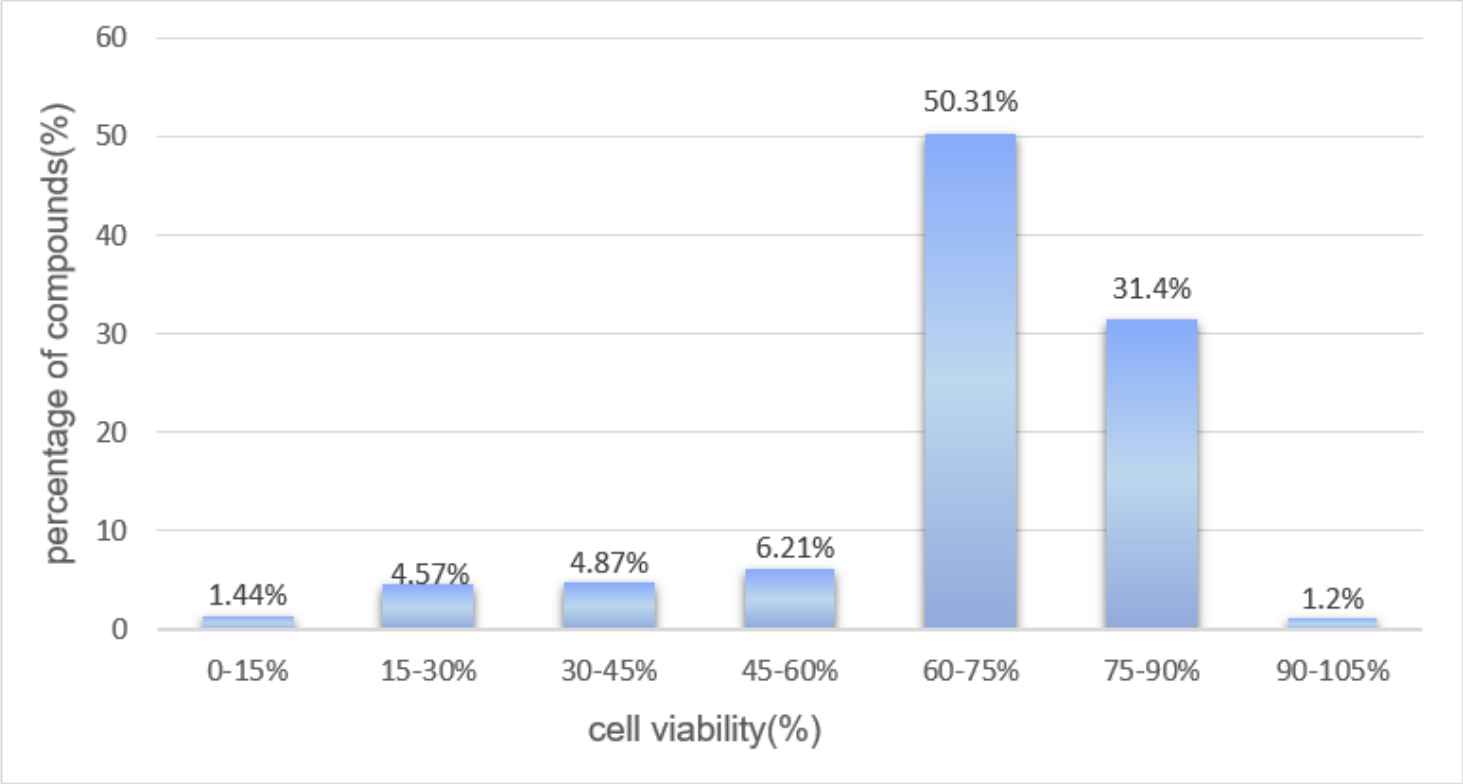

Figure 3

The percentage of compounds with different viability on BV2 cell LPS model in the chemical screening. The screening was repeated once

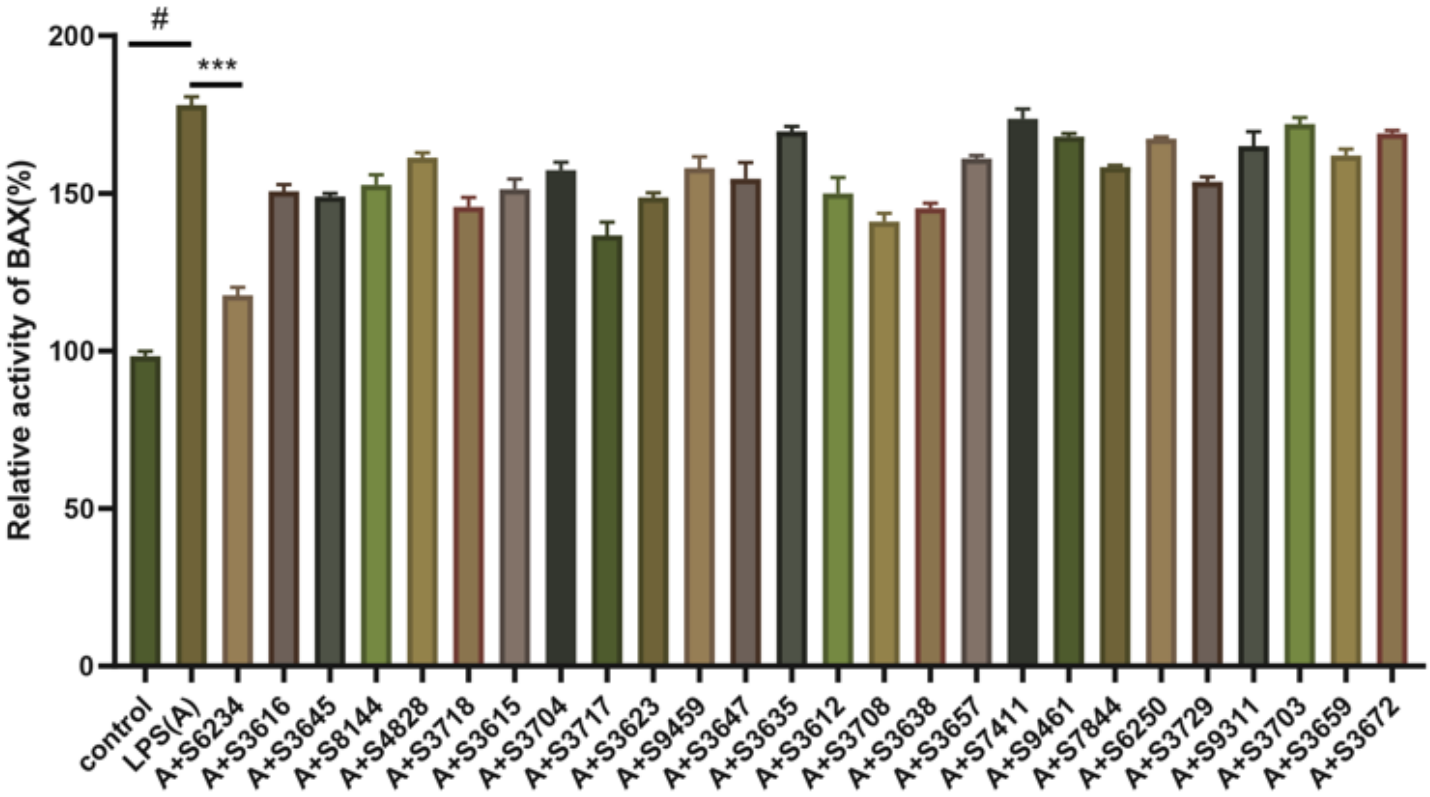

Figure 4

BAX activity was used as an indicator of secondary screening. The expression levels of BAX on LPS model treated with 26 molecule compounds (#P<0.001 compared with control group, and ***P<0.001 compared with LPS+Reb B group, n=3 in each group)

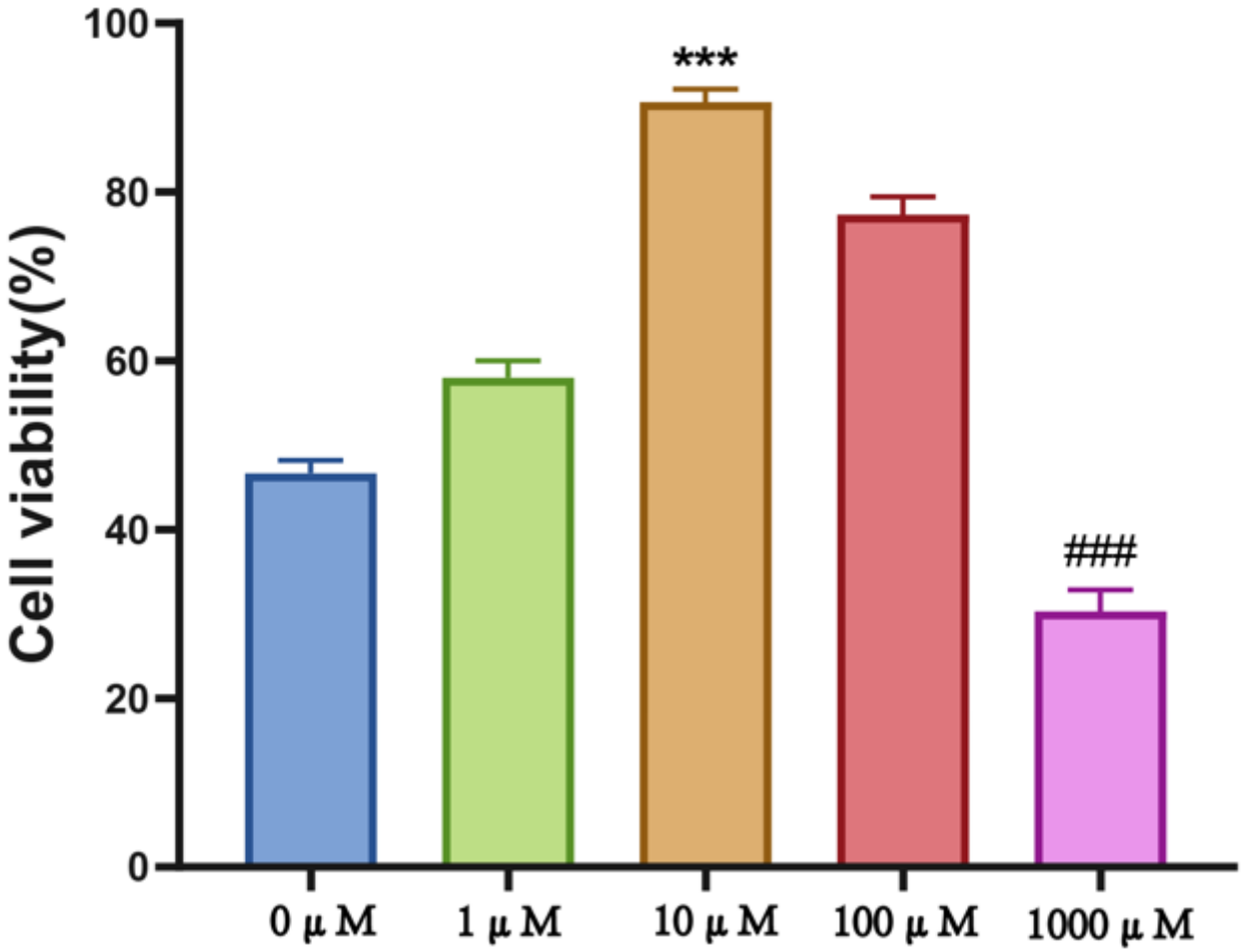

Figure 5

The cell viability after Reb B intervention with different concentration gradients (***P<0.001 compared with control group and ###P<0.001 compared with LPS group, n =3 in each group)

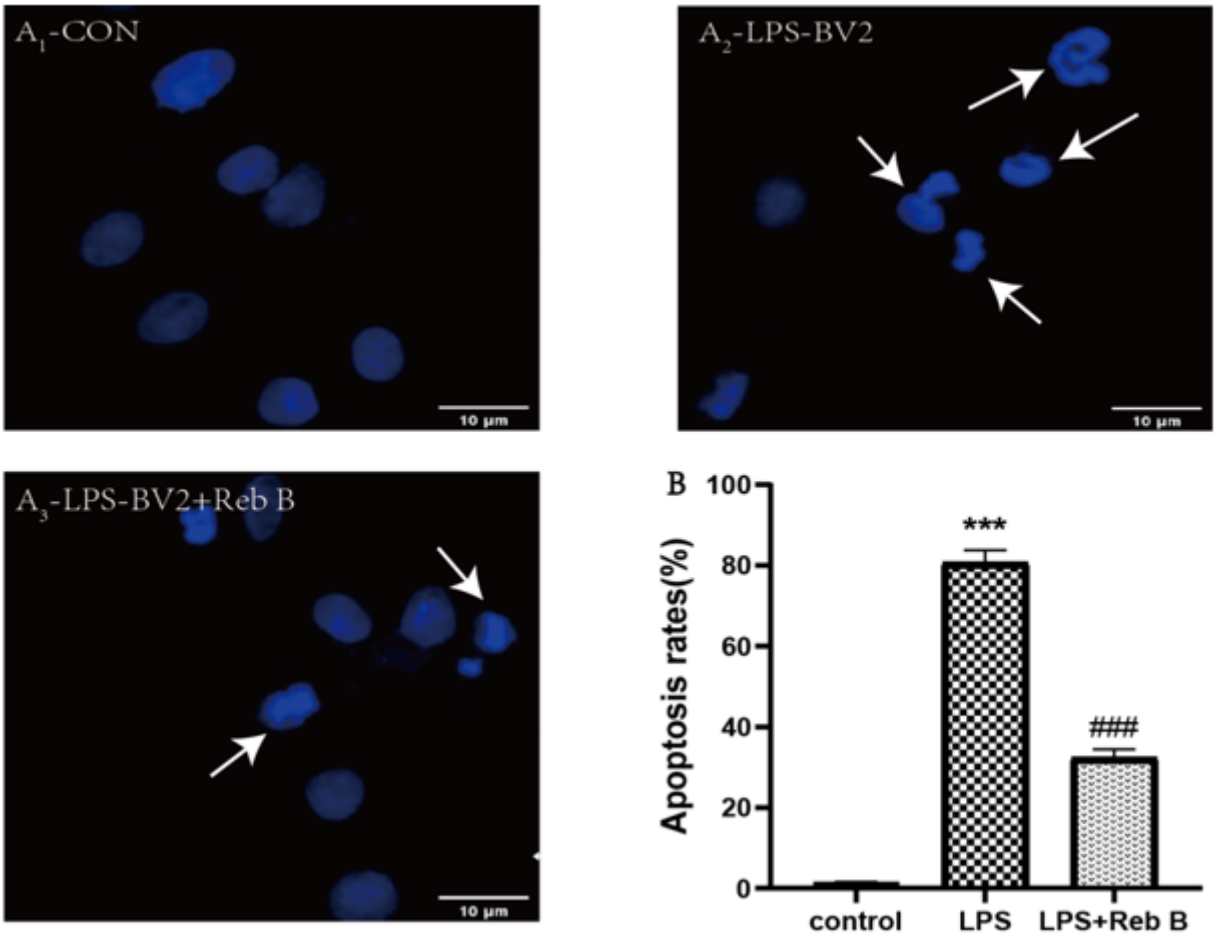

Figure 6

After the Reb B intervention, Hoechest 33258 staining was performed on BV2 cells in each group. (A) Hoechest 33258 staining demonstrated the morphology of BV2 cells in each group, (B) The apoptosis rates in the control group, LPS group,LPS+Reb B group (***P<0.001 compared with control group and ###P<0.001 compared with LPS group, n =3 in each group)

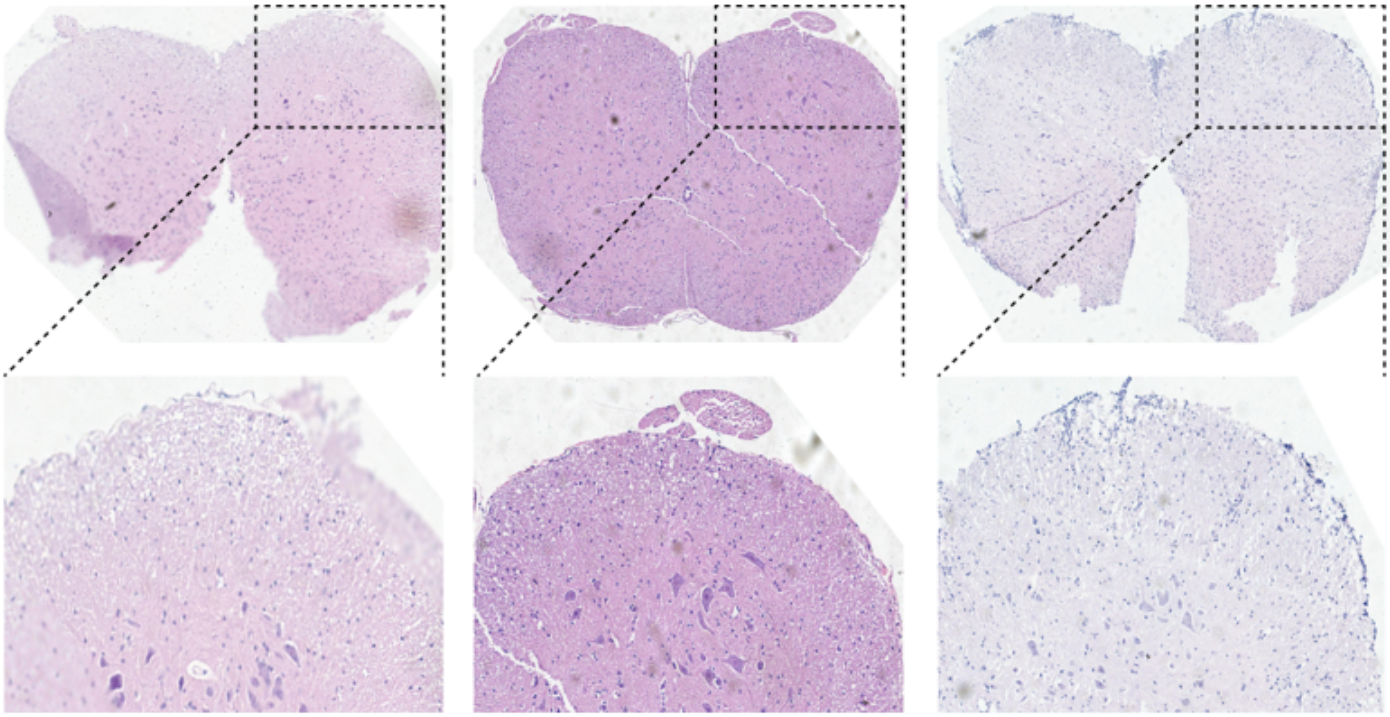

Figure 7

Infiltration of inflammatory cells as analyzed by H&E staining (40×and 200×)

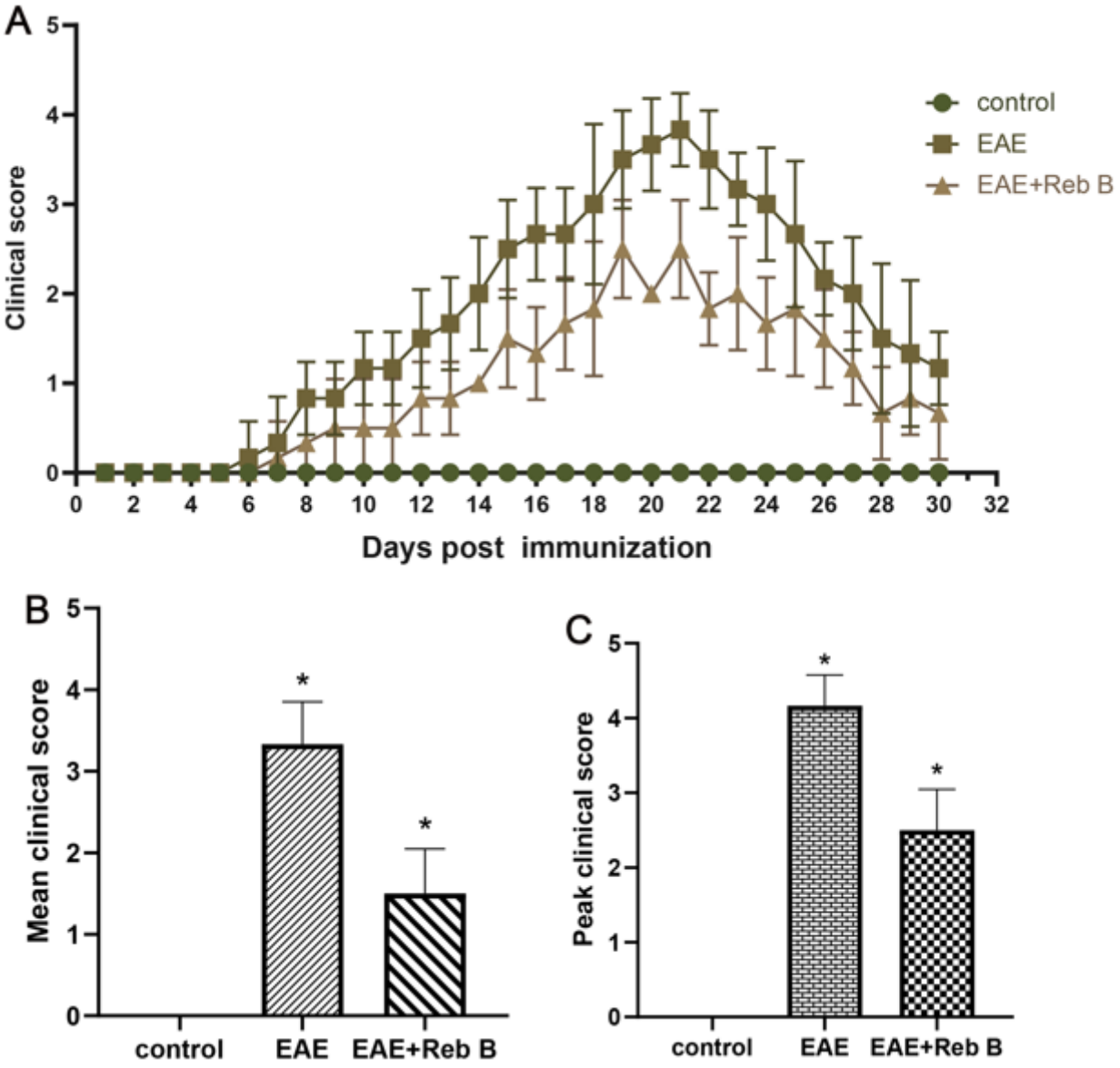

Figure 8

Symptom scoring of mice after immunization (A) Comparison of the clinical scores of the EAE group, the Reb B group and the control group. For clinical scores, n=10 mice per group. (B) and (C) showed bar graphs of the mean clinical symptom scores and highest symptom scores for each group of mice (* $P < 0.05$ compared with the control group)

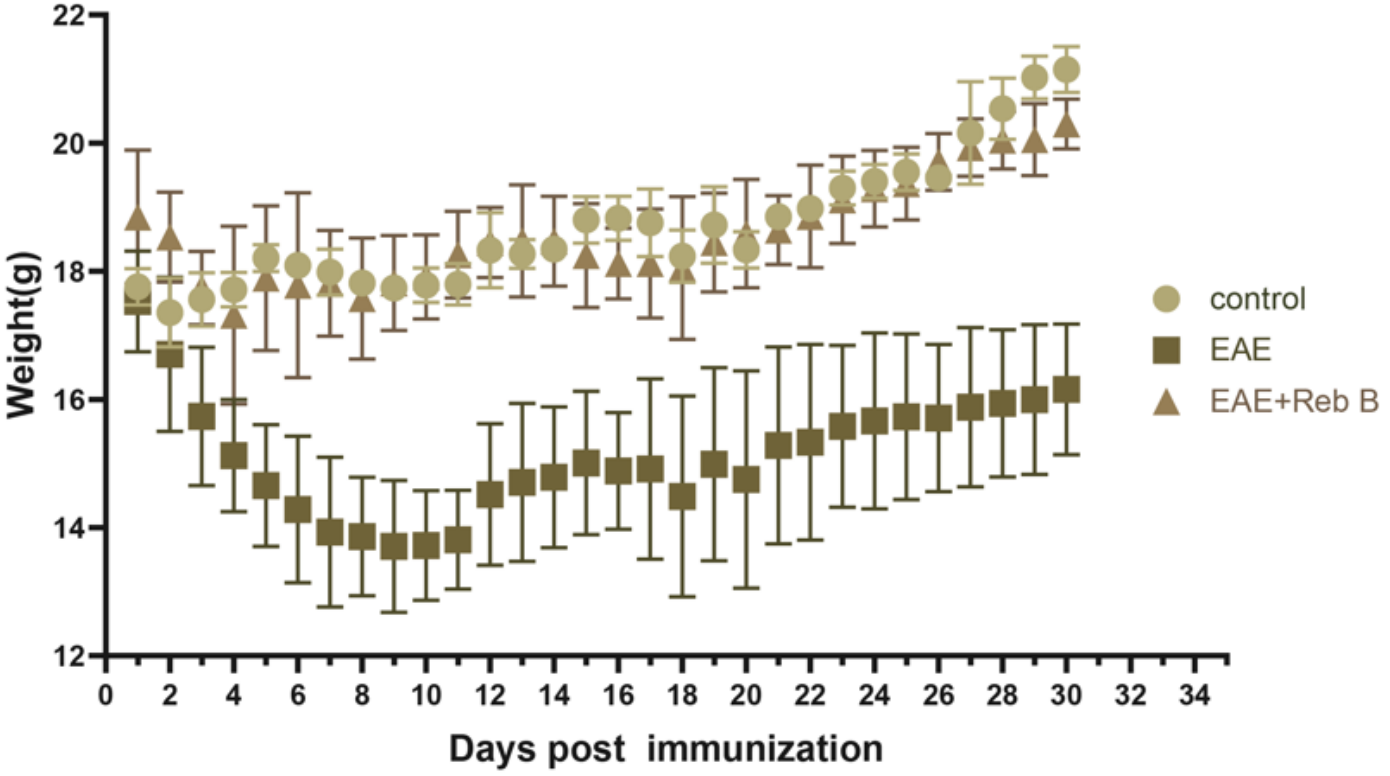

Figure 9

The weight change of each group

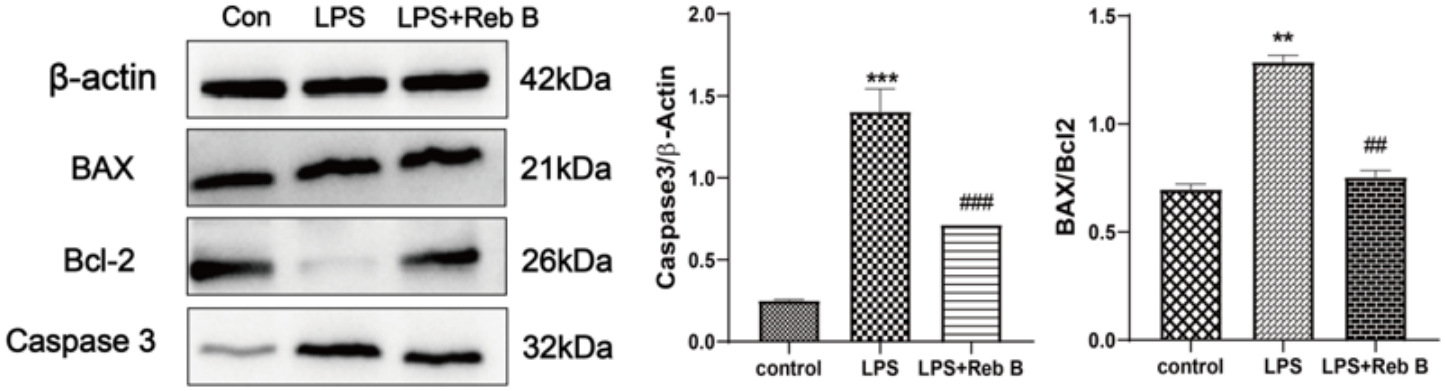

Figure 10

The expression of Caspase3, Bax and Bcl2 in the control group, LPS group, and the LPS+Reb B group was analyzed by Western blot, (***P < 0.001, ***P < 0.001, **P < 0.01 compared with Control ,and ###P < 0.001, ##P < 0.01 compared with LPS group, n =3 in each group)

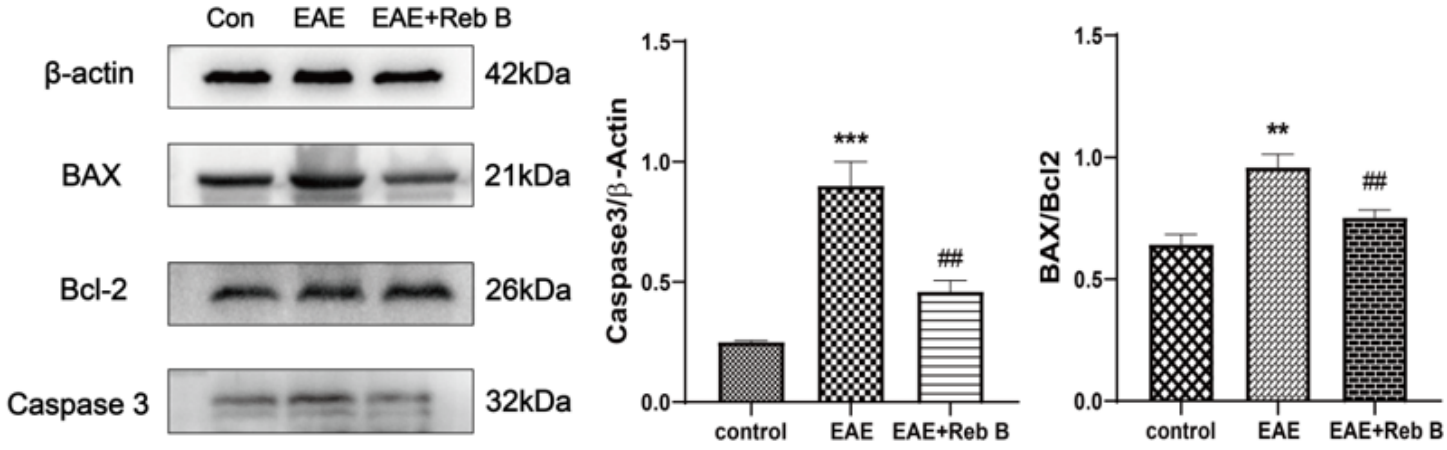

Figure 11

The expression of Caspase3, Bax and Bcl2 in the control group, LPS group, and the LPS+Reb B group was analyzed by Western blot

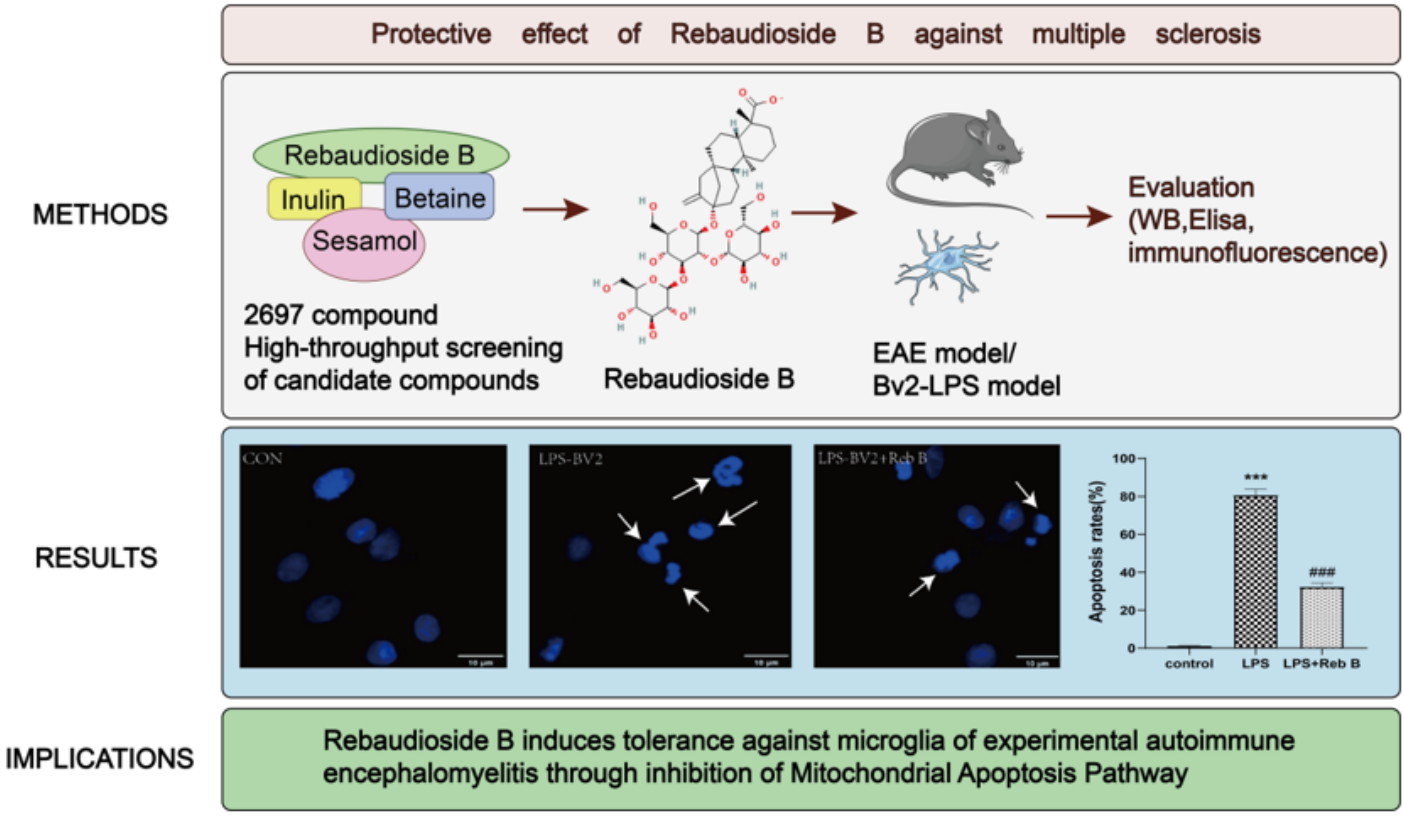

Figure 12

The overall framework of the study